Pursuit Formations of Unicycles ⋆

Joshua A. Marshall [a], Mireille E. Broucke [a], Bruce A. Francis [a]

[a] *Systems Control Group, Department of Electrical and Computer Engineering*
University of Toronto, 10 King's College Rd, Toronto, ON M5S 3G4 Canada

Abstract

In this paper, the stability of equilibrium formations for multiple unicycle systems in cyclic pursuit is studied in detail. The cyclic pursuit setup is particularly simple in that each unicycle i pursues only one other unicycle, unicycle $i+1$ (modulo n), where n is the number of unicycles. This research is principally motivated by the historical development of pursuit problems found in the mathematics and science literature, which dates as far back as 1732 and yet continues to be of current interest. On the other hand, it is anticipated that the analytical techniques and solutions pertaining to these problems will prove relevant to the study of multiagent systems and in cooperative control engineering.

Key words: Multiagent systems, Cooperative control, Circulant matrices, Pursuit problems.

1 Introduction

Problems based on the notion of *pursuit* have appealed to the curiosity of mathematicians and scientists over a period spanning centuries. These ideas apparently originated in the mathematics of *pursuit curves* (c. 1732), first studied by French scientist Pierre Bouguer [2]. Simply put, if a point a in space moves along a known curve, then another point p describes a pursuit curve if the motion of p is always directed towards a and the two points move with equal speeds. More than a century later, in 1877, Edouard Lucas asked, what trajectories would be generated if three dogs, initially placed at the vertices of an equilateral triangle, were to run one after the other? In 1880, Henri Brocard replied with the answer that each dog's pursuit curve would be that of a logarithmic spiral and that the dogs would meet at a common point, known now as the *Brocard point* of a triangle [2]. As a consequence of these old ideas, contemporary researchers have shown notable interest in problems based on the latter concept of *cyclic pursuit*, on which this paper is based.

Herein, we generalize the notion of cyclic pursuit to systems of n ordered and identical planar agents, where each individual agent i pursues the next, $i+1$ modulo n. In particular, we study the stability of equilibrium formations when the agents are modelled as unicycles. Multiagent systems and cooperative control have become topics of growing popularity within the systems engineering research community. Certainly, the possible applications for multiple cooperating agents are numerous, and include: terrestrial, space, and oceanic exploration; military surveillance and rescue; or even automated transportation systems. Therefore, from an engineering perspective, the challenging problem of how to employ only *local* interactions (e.g., pursuit) to generate *global* behaviors for the collective is of distinct interest. For a sampling and review of some recent research in multiagent and cooperative control, see [6,8,9,13,14].

1.1 The History of Pursuit

We take as inspiration for our study the historical development of cyclic pursuit problems found in the mathematics and science literature. In one of his several *Scripta Mathematica* articles on the subject, Bernhart [2] reveals an intriguing history of cyclic pursuit, beginning with Brocard's response to Lucas in 1880. Among his findings, Bernhart reported on a *Pi Mu Epsilon* talk given by a man named Peterson, who apparently extended the original three dogs problem to n ordered "bugs" that start at the vertices of a regular n-polygon. He is said to have illustrated his results for the square using four "cannibalistic spiders." Thus, if each bug pursues the next modulo n (i.e., *cyclic* pursuit) at fixed speed, the bugs will trace out logarithmic spirals and eventually

⋆ This paper was not presented at any IFAC meeting. Corresponding author Joshua A. Marshall. Tel. +1-416-978-6289. Fax +1-416-978-0804.

Email addresses: marshall@control.toronto.edu (Joshua A. Marshall), broucke@control.toronto.edu (Mireille E. Broucke), francis@control.toronto.edu (Bruce A. Francis).

meet at the polygon's centre. Ref. [17] provides a solution to this regular n-bugs problem, also noting that the constant speed assumption is not necessary.

Suppose the bugs do not start at the vertices of a regular n-polygon. Ref. [11] shows that, for three bugs, so long as the bugs are not initially arranged so that they are all collinear, they will meet at a common point and this meeting will be mutual. The n-bug problem was later examined by the authors of [1], who proved that "a bug cannot capture another bug which is not capturing another bug [i.e., *mutual* capture], except by head-on collision." They used their result to show that, specifically for the 4-bugs problem, the terminal capture is indeed mutual. Very recently, Richardson [15] resolved this issue for n-bugs, showing "it is possible for bugs to capture their own prey without all bugs simultaneously doing so, even for non-collinear initial positions." However, he also proved that if these initial positions are chosen randomly, then the probability that a non-mutual capture will occur is zero. Other variations on the traditional cyclic pursuit problem have also been considered. For example, [3] studies both continuous and discrete pursuit problems, as well as both constant and varying speed scenarios. For a more complete review, see [2,15].

1.2 Agents in Cyclic Pursuit

Suppose we now imagine that each "bug" is instead an autonomous agent in the plane. In what follows, we generalize the cyclic pursuit concept to autonomous agents and discuss its properties as a possible coordination framework for multiagent systems. In particular, we consider the case when each agent is subject to a single nonholonomic motion constraint, or equivalently, modelled as a unicycle. Therefore, depending on the allowed control energy, each agent will require some finite time to steer itself towards its prey. What global motions can be generated? We first asked this question in [12], where preliminary results appeared. Recently, the author of [16] posed a similar question for a particular constant speed version of the n-bugs problem. He showed that the system's limiting behavior exponentially resembles a *regular* n-polygon, but only when $n \geq 7$.

Thus, our primary motivation is to follow historical development and study the achievable formations for unicycles under cyclic pursuit. Then again, practically speaking, the study of cyclic pursuit may result in a feasible strategy for multiple vehicle systems since it is distributed (i.e., decentralized and there is no leader) and rather simple in that each agent is required to sense information from only one other agent. Our study begins by classifying all possible equilibrium formations for unicycles in cyclic pursuit. We first state the results of a global stability analysis for the case when $n = 2$, which originally appeared in [12], followed by a complete local stability analysis for the general case when $n \geq 2$. Moreover, in each case it is exposed how the multiple unicycle system's global behavior can be changed by appropriate controller gain assignments.

2 Cyclic Pursuit Equations

In the classical n-bugs problem, a standard approach [3,15] is to formulate the problem using a differential equation model for each agent. For example, consider n ordered and identical mobile agents in the plane, their positions at each instant denoted $z_i = (x_i, y_i) \in \mathbb{R}^2$, $i = 1, 2, \ldots, n$. Suppose the kinematics of each agent are described by an integrator $\dot{z}_i = u_i$, with control inputs $u_i = k(z_{i+1} - z_i)$, so that each agent i effectively pursues the next $i + 1$ modulo [1] n. Thus, the well known result, proven formally in [3], is as follows.

Theorem 1 (Linear Pursuit) *Consider n agents in $\mathbb{R}^2$ with kinematics $\dot{z}_i = u_i$ and control inputs $u_i = k(z_{i+1} - z_i)$, where $k > 0$. For every initial condition, the centroid of the agents $z_1(t), z_2(t), \ldots, z_n(t)$ remains stationary and every agent $z_i(t)$, $i = 1, 2, \ldots, n$ exponentially converges to this centroid.*

In this paper, we extend the above *linear* cyclic pursuit scenario to one in which each agent is a kinematic unicycle with nonlinear state model

$$\begin{bmatrix} \dot{x}_i \\ \dot{y}_i \\ \dot{\theta}_i \end{bmatrix} = \begin{bmatrix} \cos\theta_i & 0 \\ \sin\theta_i & 0 \\ 0 & 1 \end{bmatrix} \begin{bmatrix} v_i \\ \omega_i \end{bmatrix}, \tag{1}$$

where $(x_i, y_i) \in \mathbb{R}^2$ denotes the i-th unicycle's Cartesian position, $\theta_i \in \mathbb{S}^1$ is the unicycle's orientation, and $u_i = (v_i, \omega_i) \in \mathbb{R}^2$ are control inputs.

Let r_i denote the distance between unicycles numbered i and $i + 1$, and let α_i be the angle from the i-th unicycle's heading to the heading that would take it directly towards unicycle $i + 1$ (see Fig. 1). In analogy with the previously described linear model, an intuitive control law for unicycles is to assign unicycle i's linear speed v_i in proportion to r_i, while assigning its angular speed ω_i in proportion to α_i. It is this cyclic pursuit strategy that is analyzed in this paper.

2.1 Transformation to Relative Coordinates

To facilitate the analysis, it is useful to consider a transformation to (relative) coordinates involving the variables r_i, α_i, and β_i (see Fig. 1). After some algebraic

[1] Henceforth, all agent indices $i + 1$ should be evaluated modulo n (i.e., *cyclic* pursuit), unless stated otherwise.

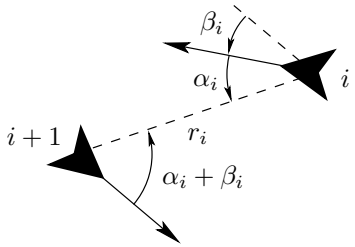

Fig. 1. New coordinates, with unicycle i in pursuit of $i+1$.

manipulation (see [12]), the equations become

$$\begin{aligned}\dot{r}_i &= -v_i \cos\alpha_i - v_{i+1}\cos(\alpha_i+\beta_i)\\ \dot{\alpha}_i &= \frac{1}{r_i}\left(v_i \sin\alpha_i + v_{i+1}\sin(\alpha_i+\beta_i)\right) - \omega_i \qquad (2)\\ \dot{\beta}_i &= \omega_i - \omega_{i+1}.\end{aligned}$$

This system describes the relationship between unicycle i and the one that it is pursuing, $i+1$. Note that, in these coordinates, it is assumed that $r_i > 0$. One might also observe that the transformation from $q_i = (x_i, y_i, \theta_i)$ into $\xi_i = (r_i, \alpha_i, \beta_i)$ is not invertible, which is not surprising since we have removed any reference to a global coordinate frame. In what follows, we keep the ensuing redundancy in (2) as it allows us to exploit the cyclic interconnection structure of the problem.

2.2 Formation Control and the Pursuit Graph

At each instant, regardless of the control law, the multiple unicycle system's geometric arrangement in the plane can be described by a *pursuit graph*.

Definition 2 (Pursuit Graph) *A* pursuit graph G *consists of a pair* (V, E) *such that (i)* V *is a finite set of vertices,* $|V| = n$*, where each vertex* $z_i = (x_i, y_i) \in \mathbb{R}^2$*,* $i \in \{1, \ldots, n\}$*, represents the position of unicycle* i *in the plane; and (ii)* E *is a finite set of directed edges,* $|E| = n$*, where each edge* $e_i : V \times V \to \mathbb{R}^2$*,* $i \in \{1, \ldots, n\}$*, is the vector from* z_i *to its prey,* z_{i+1}*.*

In other words, $e_i = z_{i+1} - z_i$ and consequently $\sum_i^n e_i = 0$ for unicycles in cyclic pursuit. Also, note that our coordinate $r_i \equiv \|e_i\|_2$. In the next section, we use this definition to characterize the equilibrium formations of our multiple unicycle system. As previously discussed, this paper studies the case when the control inputs are

$$v_i = k_r r_i \text{ and } \omega_i = k_\alpha \alpha_i, \qquad (3)$$

where $k_r, k_\alpha > 0$ are constant gains (see [13] for the very different case when v_i is constant). Using these control inputs, we obtain via (2) a system of n cyclically interconnected and identical subsystems

$$\dot{r}_i = -k_r\left(r_i \cos\alpha_i + r_{i+1}\cos(\alpha_i+\beta_i)\right) \qquad (4a)$$

$$\dot{\alpha}_i = k_r\left(\sin\alpha_i + \frac{r_{i+1}}{r_i}\sin(\alpha_i+\beta_i)\right) - k_\alpha\alpha_i \qquad (4b)$$

$$\dot{\beta}_i = k_\alpha(\alpha_i - \alpha_{i+1}). \qquad (4c)$$

See [12] for details concerning the derivation of (4).

Preliminary computer simulations suggest the possibility of achieving circular pursuit trajectories in the plane. Fig. 2 shows results for a system of $n = 5$ unicycles, initially positioned at random, where the gain $k_\alpha = 1$ is fixed but gain $k_r = k^* := \frac{\pi}{10}\csc\left(\frac{\pi}{5}\right)$, after (5). In this case, the unicycles converge to evenly spaced motion around a circle with a pursuit graph that appears similar to a regular pentagon. In Fig. 3 and Fig. 4, the unicycles converge to a point and diverge, respectively, while at the same time approaching evenly spaced motion that resembles a regular pentagon.

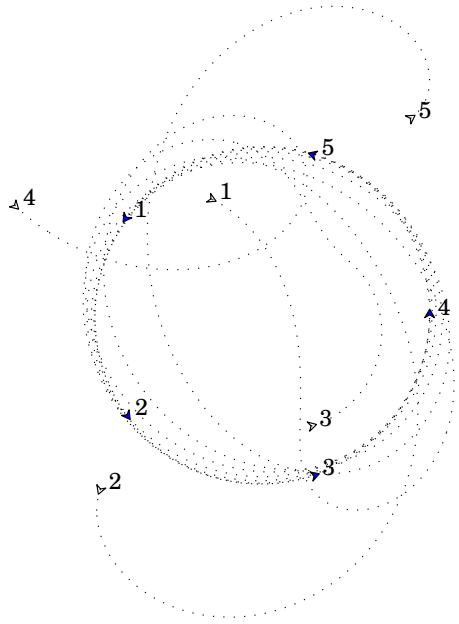

Fig. 2. Five unicycles, $k_\alpha = 1$, $k_r = k^*$.

3 Formation Equilibria

In this section, we analyze the system of interconnected unicycles (4) to determine the possible equilibrium formations under control law (3). We define equilibrium with reference to (4); that is, ξ_i is constant for all $i = 1, 2, \ldots, n$. In other words, to each unicycle the others appear stationary. Towards achieving this goal, we need to adequately describe the state of our system's pursuit graph at equilibrium. The following definition for a planar polygon has been adapted from [4] to allow for possibly coincident vertices and for directed edges.

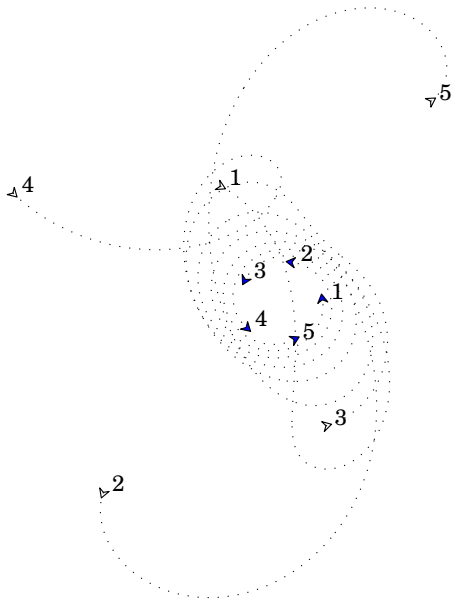

Fig. 3. Five unicycles, $k_\alpha = 1$, $k_r < k^*$.

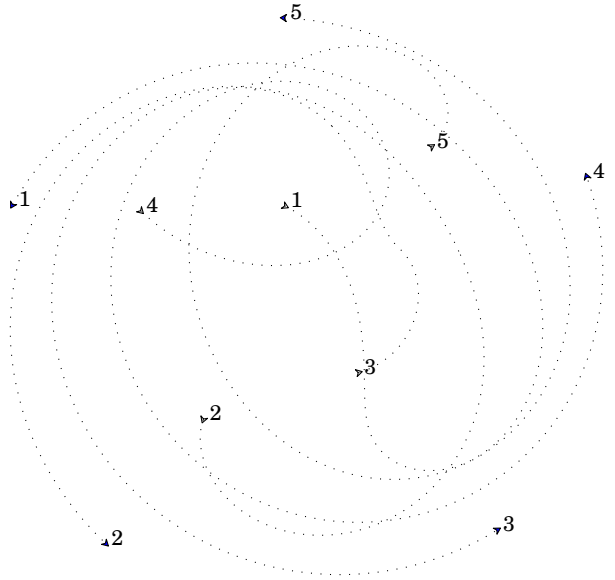

Fig. 4. Five unicycles, $k_\alpha = 1$, $k_r > k^*$.

Definition 3 (after [4], p. 93) *Let n and $d < n$ be positive integers so that $p := n/d > 1$ is a rational number. Let R be the positive rotation in the plane, about the origin, through angle $2\pi/p$ and let $z_1 \neq 0$ be a point in the plane. Then, the points $z_{i+1} = Rz_i$, $i = 1, \ldots, n-1$ and edges $e_i = z_{i+1} - z_i$, $i = 1, \ldots, n$, define a* generalized regular polygon*, which is denoted $\{p\}$.*

Since p is rational, the period of R is finite and, when n and d are coprime, this definition is equivalent to the well-known definition of a regular polygon as a polygon that is both *equilateral* and *equiangular* [4]. Moreover, when $d = 1$, $\{p = n\}$ is an *ordinary* regular polygon (i.e., its edges do not cross one another). However, when $d > 1$ is coprime to n, $\{p\}$ is a *star* polygon since its sides intersect at certain extraneous points, which are not included among the vertices [4, pp. 93–94]. If n and d have a common factor $m > 1$, then $\{p\}$ has $\tilde{n} = n/m$ distinct vertices and $\tilde{n}$ edges traversed m times. Note that the trivial case when $d = n$ has not been included since this corresponds to the geometrically uninteresting situation where the vertices are all coincident (i.e., $r_i = 0$ for all i). However, in section 6 we do consider the stability of such a point. Fig. 5 illustrates some possibilities for $\{p\}$ when $n = 9$. In the first instance, $\{9/1\}$ is an ordinary polygon. In the second instance, $\{9/2\}$ is a star polygon since 9 and 2 are coprime. In the last case, the edges of $\{9/3\}$ traverse a $\{3/1\}$ polygon 3 times, because $m = 3$ is a common factor of both 9 and 3.

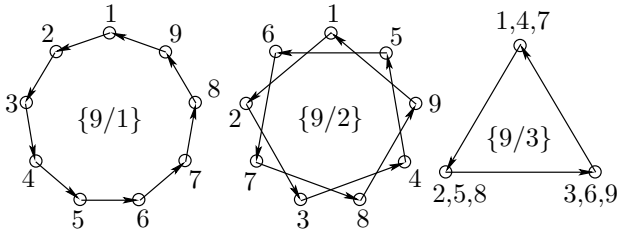

Fig. 5. Generalized regular polygons $\{9/d\}$, $d \in \{1, 2, 3\}$.

Lemma 4 (after [4], p. 94) *The internal angle at every vertex of $\{p\}$ is given by $\psi = \pi\,(1 - 2d/n)$.*

Our first theorem, which originally appeared in [12], reveals the set of possible equilibrium formations for our system of n unicycles in cyclic pursuit.

Theorem 5 *At equilibrium, the n-unicycle pursuit graph corresponding to (4) is a generalized regular polygon $\{p\}$, where $p = n/d$ and $d \in \{1, \ldots, n-1\}$. Consequently, for all $i = 1, 2, \ldots, n$, the equilibrium values for α_i and β_i in the range $[-\pi, \pi)$ are $(\bar{\alpha}, \bar{\beta}) = \left(\frac{\pi d}{n}, \pi - \frac{2\pi d}{n}\right)$ for positively oriented motion, and $(\bar{\alpha}, \bar{\beta}) = \left(-\frac{\pi d}{n}, \frac{2\pi d}{n} - \pi\right)$ for negatively oriented motion. In each case, $r_i = \bar{r} > 0$ is a constant.*

The case when n and d of Theorem 5 are not coprime is physically undesirable (e.g., as in $\{9/3\}$ of Fig. 5) since it requires that multiple unicycles occupy the same point in space. From geometry, it is clear that, for each possible $\{n/d\}$ formation, $\bar{\alpha} = \pm\pi\frac{d}{n}$ corresponds exactly to a relative heading for each unicycle that points it in a direction that is *tangent* to the circle circumscribed by the vertices of the corresponding polygon.

At equilibrium, (4b) simplifies to

$$\begin{aligned} k_r/k_\alpha &= \bar{\alpha}\left(\sin\bar{\alpha} + \sin(\bar{\alpha} + \bar{\beta})\right)^{-1} \\ &= \frac{\pi d}{2n}\csc\left(\frac{\pi d}{n}\right) =: k^*. \end{aligned} \tag{5}$$

In other words, the ratio k^* must be as defined in order that an equilibrium (with equilibrium distance $\bar{r} > 0$) exists. Thus, without loss of generality, we can choose $k_\alpha = 1$ and $k_r = k^*$ to ensure the existence of regular polygon equilibria. For example, an equilibrium formation $\{5/1\}$ has $k^* = \frac{\pi}{10}\csc\left(\frac{\pi}{5}\right)$, corresponding to the gain used to generate the simulation results of Fig. 2.

3.1 Global Stability Analysis for $n = 2$

In general, when $n > 2$ a global stability analysis of the multiple unicycle system (4) is not an easy task. However, when $n = 2$ the analysis is simplified in that $r_1 = r_2$, $\alpha_2 = \alpha_1 + \beta_1$, and $\alpha_1 = \alpha_2 + \beta_2$. By choosing $k_\alpha = 1$ and $k_r = k > 0$, (4) reduces to

$$\begin{aligned}
\dot{r}_1 &= -kr_1\left(\cos\alpha_1 + \cos(\alpha_1 + \beta_1)\right) && \text{(6a)}\\
\dot{\alpha}_1 &= k\left(\sin\alpha_1 + \sin(\alpha_1 + \beta_1)\right) - \alpha_1 && \text{(6b)}\\
\dot{\beta}_1 &= -\beta_1 && \text{(6c)}\\
\dot{r}_2 &= -kr_2\left(\cos\alpha_2 + \cos(\alpha_2 + \beta_2)\right)\\
\dot{\alpha}_2 &= k\left(\sin\alpha_2 + \sin(\alpha_2 + \beta_2)\right) - \alpha_2\\
\dot{\beta}_2 &= -\beta_2.
\end{aligned}$$

Since the unicycle equations are decoupled, we drop the indices to simplify notation and proceed by analyzing (6). The behavior of this two-unicycle system depends on the choice of gain k. However, observe that when $\beta(0) = -2\alpha(0)$, subsystems (6b) and (6c) respectively reduce to $\dot{\alpha} = -\alpha$ and $\dot{\beta} = -\beta$ for all $t \geq 0$, independent of any particular choice for k. Moreover, it can be verified that, given (6), $r(t) > 0$ holds for all $t \geq 0$.

Theorem 6 *Consider $n = 2$ unicycles in cyclic pursuit, each with kinematics (6). Let $\mathcal{W} = \{\xi = (\alpha, \beta) : \beta = -2\alpha\}$ and $k^* = \frac{\pi}{4}$ after (5). Then, (i) if $0 < k < k^*$ or if $\xi(0) \in \mathcal{W}$ and $0 < k < \frac{5\pi}{4}$, the unicycles converge to a common point; (ii) if $k^* < k < \frac{5\pi}{4}$ and $\xi(0) \notin \mathcal{W}$, the unicycles diverge, or; (iii) if $k = k^*$ and $\xi(0) \notin \mathcal{W}$, the unicycles converge to equally spaced circular motion.*

A proof of Theorem 6 can be found in [12]. Whether the unicycles circle each other in the counterclockwise or clockwise direction depends on their relative initial conditions, as detailed in [12]. Also, the set of initial conditions $\xi(0) \in \mathcal{W}$, for which changes in k have no effect corresponds to unicycles that start with $\alpha_1(0) = \alpha_2(0) + \beta_2(0) = -\alpha_2(0)$ (see Fig. 6a). Fig. 6b shows the special case when $\alpha_1(0) = \alpha_2(0) = 0$. Fig. 6c illustrates the case when $\alpha_1(0) = \pi$ and $\alpha_2(0) = -\pi$. Note that the same geometric arrangement can be described by $\alpha_1(0) = \alpha_2(0) = \pi$. However, in this case the unicycles' behavior depends on the chosen gain k.

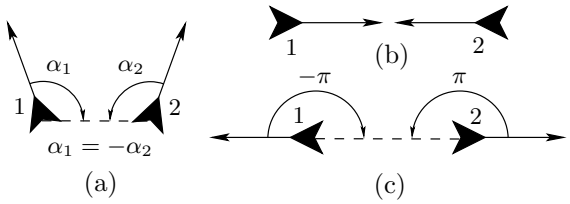

Fig. 6. Possible configurations for $\xi(0) \in \mathcal{W}$.

4 Geometry of Pursuit

In the general case, when $n \geq 2$, the number of equilibrium formations $\{n/d\}$ increases with n, making a global analysis very difficult. On the other hand, it is possible to study the *local* stability properties of these equilibria via linearization. Thus, the problem is to determine, for a given number of unicycles n, which $\{n/d\}$ equilibrium polygons are stable and which are not. Furthermore, we are interested in understanding how the gains k_r and k_α influence the system's steady-state behavior.

To facilitate notation, let $\xi_i = (r_i, \alpha_i, \beta_i) \in \mathbb{R}^3$ so that the kinematics of each unicycle subsystem (4) can be written more compactly as $\dot{\xi}_i = f(\xi_i, \xi_{i+1})$. Moreover, let $\xi = (\xi_1, \xi_2, \ldots, \xi_n) \in \mathbb{R}^{3n}$ so that the complete multiple unicycle system may be viewed as the autonomous nonlinear system

$$\dot{\xi} = \hat{f}(\xi). \qquad (7)$$

Let $\hat{A}$ denote the Jacobian of $\hat{f}$, evaluated at an equilibrium formation. Before linearizing (7) about a given equilibrium formation, it is possible to make some key geometric observations about the possible trajectories of (7). These results prove useful in the sections that follow, when interpreting the spectrum of $\hat{A}$ for the linearized multiple unicycle system.

4.1 Pursuit Constraints

The first relevant geometric observation is that, for every initial condition, the system (7) is constrained to evolve on a submanifold $\mathcal{M}$ of $\mathbb{R}^{3n}$ that is invariant under $\hat{f}$. To see why this is the case, recall that, by the definition of e_i, the system's pursuit graph at each instant must satisfy $\sum_{i=1}^{n} e_i(t) = 0$. By choosing, without loss of generality, a coordinate frame attached to unicycle 1 and oriented with this unicycle's heading, this condition corresponds to trajectory constraints described by the equations

$$\begin{aligned}
g_1(\xi) = {} & r_1\sin\alpha_1 + r_2\sin(\alpha_2 + \pi - \beta_1)\\
& + r_3\sin(\alpha_3 + 2\pi - \beta_1 - \beta_2) + \cdots\\
& \cdots + r_n\sin(\alpha_n + (n-1)\pi - \textstyle\sum_{i=1}^{n-1}\beta_i) = 0\\
g_2(\xi) = {} & r_1\cos\alpha_1 + r_2\cos(\alpha_2 + \pi - \beta_1)\\
& + r_3\cos(\alpha_3 + 2\pi - \beta_1 - \beta_2) + \cdots\\
& \cdots + r_n\cos(\alpha_n + (n-1)\pi - \textstyle\sum_{i=1}^{n-1}\beta_i) = 0.
\end{aligned}$$

Using unicycles 1 and 2, for example, Fig. 7 helps to illustrate how these equations arise.

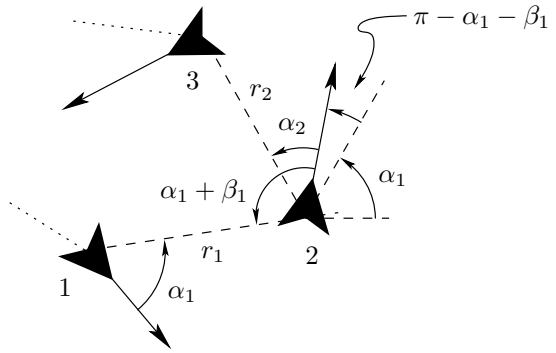

Fig. 7. Depiction of coordinates for unicycles 1 and 2.

Also, from (4c) $\sum_{i=1}^n \dot{\beta}_i(t) = 0 \implies \sum_{i=1}^n \beta_i(t) \equiv c$ for all $t \geq 0$, where $c = -n\pi$ by our definition for $\beta_i := \theta_i - \theta_{i+1} - \pi$, which yields

$$g_3(\xi) = \sum_{i=1}^n \beta_i + n\pi = 0 \bmod 2\pi.$$

Let $g(\xi) = (g_1(\xi), g_2(\xi), g_3(\xi))$, the vector of constraint functions. Then it can be checked that $\mathcal{M} = \{\xi \in \mathbb{R}^{3n} : g(\xi) = 0\}$ defines a submanifold $\mathcal{M} \subset \mathbb{R}^{3n}$.

Lemma 7 *$\mathcal{M}$ is invariant under the flow of* (7).

Corollary 8 *Given $\bar{\xi} \in \mathcal{M}$, the tangent space $T_{\bar{\xi}}\mathcal{M}$ is an invariant subspace of the linearization at $\bar{\xi}$ of* (7).

Proofs for Lemma 7 and Corollary 8 have been omitted for brevity. Following Corollary 8, there exists a change of basis that transforms $\hat{A}$ into upper-triangular form

$$\begin{bmatrix} \hat{A}_{T_{\bar{\xi}}\mathcal{M}} & * \\ 0_{3\times(3n-3)} & \hat{A}^\star_{T_{\bar{\xi}}\mathcal{M}} \end{bmatrix}.$$

Lemma 9 *In the quotient space $\mathbb{R}^{3n}/T_{\bar{\xi}}\mathcal{M}$, the induced linear transformation $\hat{A}^\star_{T_{\bar{\xi}}\mathcal{M}} : \mathbb{R}^{3n}/T_{\bar{\xi}}\mathcal{M} \to \mathbb{R}^{3n}/T_{\bar{\xi}}\mathcal{M}$ has (imaginary axis) eigenvalues $\lambda_1 = 0$ and $\lambda_{2,3} = \pm j\bar{\alpha}$.*

PROOF. Consider new coordinates $\varphi = \Phi(\xi)$,

$$\begin{aligned} \varphi_1 = r_1, \varphi_2 = \alpha_1, \ldots, \varphi_{3n-3} = \beta_{n-1}, \\ \varphi_{3n-2} = g_1(\xi), \varphi_{3n-1} = g_2(\xi), \varphi_{3n} = g_3(\xi). \end{aligned}$$

Partition these new coordinates into $\varphi = (\varphi_{\mathrm{I}}, \varphi_{\mathrm{II}})$, where $\varphi_{\mathrm{I}} = (\varphi_1, \varphi_2, \ldots, \varphi_{3n-3})$ and $\varphi_{\mathrm{II}} = (\varphi_{3n-2}, \varphi_{3n-1}, \varphi_{3n})$.

Notice that the set of coordinates in φ_{II} are precisely the functions that define $\mathcal{M}$. Thus, in the new coordinates

$$\begin{aligned} \dot{\varphi}_{\mathrm{I}} &= \begin{bmatrix} I_{3n-3} & 0_{(3n-3)\times 3} \end{bmatrix} \hat{f}(\xi)\Big|_{\xi=\Phi^{-1}(\varphi)} \\ \dot{\varphi}_{\mathrm{II}} &= \frac{\partial g(\xi)}{\partial \xi} \hat{f}(\xi)\Big|_{\xi=\Phi^{-1}(\varphi)}. \end{aligned}$$

Moreover, the equilibrium $\bar{\varphi} = \Phi(\bar{\xi})$ is equal to $\bar{\xi}$, except that the last 3 components are instead zero. By computing the linearization about this equilibrium one obtains

$$\begin{aligned} \dot{\varphi}_{\mathrm{I}} &= \begin{bmatrix} I_{3n-3} & 0_{(3n-3)\times 3} \end{bmatrix} \hat{A}\varphi \\ \dot{\varphi}_{\mathrm{II}} &= \frac{\partial}{\partial \varphi} \left[\frac{\partial g(\xi)}{\partial \xi} \hat{f}(\xi) \right]_{\xi=\Phi^{-1}(\varphi)} \Bigg|_{\bar{\varphi}} \varphi \\ &\overset{(*)}{=} \frac{\partial}{\partial \varphi} \begin{bmatrix} -\varphi_2\varphi_{3n-1} - k\varphi_1 \sin\varphi_{3n} \\ \varphi_2\varphi_{3n-2} + k\varphi_1 \cos\varphi_{3n} - k^*\varphi_1 \\ 0 \end{bmatrix} \Bigg|_{\bar{\varphi}} \varphi \\ &= \left[\begin{array}{ccc|ccc} 0 & \cdots & 0 & 0 & -\bar{\alpha} & -k\bar{r} \\ 0 & \cdots & 0 & \bar{\alpha} & 0 & 0 \\ 0 & \cdots & 0 & 0 & 0 & 0 \end{array}\right] \varphi \\ &= \begin{bmatrix} 0_{3\times(3n-3)} & \hat{A}^\star_{T_{\bar{\xi}}\mathcal{M}} \end{bmatrix} \varphi, \end{aligned}$$

where a derivation of the equivalence $(*)$ has been omitted for brevity. The 3×3 block $\hat{A}^\star_{T_{\bar{\xi}}\mathcal{M}}$ has eigenvalues $\lambda_{1,2,3} = \{0, \pm j\bar{\alpha}\}$, which concludes the proof.

Thus, when determining the stability of a given $\{n/d\}$ formation we can disregard these imaginary axis eigenvalues of $\hat{A}$ and conclude stability based on its remaining $3n-3$ eigenvalues. Again, this is because our system is constrained to evolve, at $\bar{\xi}$, along the tangent space $T_{\bar{\xi}}\mathcal{M} \subset \mathbb{R}^{3n}$ and not in the quotient space $\mathbb{R}^{3n}/T_{\bar{\xi}}\mathcal{M}$ corresponding to the above imaginary axis eigenvalues.

4.2 Formation Subspace

The second geometric observation about the trajectories of (7) is that there exists a *set* of points in $\mathbb{R}^{3n}$, denoted $\mathcal{E}$, where the pursuit graph G corresponding to (7) is a generalized regular polygon; we call $\mathcal{E}$ a *formation subspace*. To see this, let $k_r, k_\alpha > 0$ and constant angles $\bar{\alpha}, \bar{\beta} \in [-\pi, \pi)$ satisfy

$$k_r/k_\alpha = \bar{\alpha}\left(\sin\bar{\alpha} + \sin(\bar{\alpha} + \bar{\beta})\right)^{-1}. \tag{8}$$

Now, define a 1-dimensional affine subspace of $\mathbb{R}^{3n}$, $\mathcal{E} = \{\xi \in \mathbb{R}^{3n} : r_i = r_{i+1} \text{ for } i = 2, 3, \ldots, n, \alpha_i = \bar{\alpha} \text{ and } \beta_i =$

$\bar{\beta}$ for $i = 1, 2, \ldots, n\}$. Alternatively, $\mathcal{E}$ can be defined by $3n-1$ constraints

$$g_1(\xi) = \alpha_1 - \bar{\alpha}, g_2(\xi) = \beta_1 - \bar{\beta}, g_3(\xi) = r_2 - r_3,$$
$$g_4(\xi) = \alpha_2 - \bar{\alpha}, \ldots, g_{3n-1} = \beta_n - \bar{\beta}.$$

Lemma 10 *$\mathcal{E}$ is invariant under* (7)*.*

The proof has been omitted for brevity. In Theorem 5, we saw that at equilibrium the pursuit graph G corresponding to (7) is a generalized regular polygon $\{n/d\}$. Next, we show that G is in fact a generalized regular polygon for every $\xi \in \mathcal{E}$. However, it should be emphasized that not all of the points in $\mathcal{E}$ are equilibria.

Lemma 11 *For $\xi \in \mathcal{E}$, the n-unicycle pursuit graph G corresponding to* (7) *is a generalized regular polygon $\{p\}$, where $p = n/d$ and $d \in \{1, 2, \ldots, n-1\}$.*

The proof has been omitted. Lemma 11 says that for every n there are associated affine subspaces, henceforth denoted $\mathcal{E}_d$ where $d \in \{1, 2, \ldots, n-1\}$, each one invariant under (7) and in which the pursuit graph G corresponding to (7) is a generalized polygon of type $\{n/d\}$.

From this, we can also conclude that the constant angle $\bar{\beta}$ is always independent of the chosen gains k_r and k_α.

Corollary 12 *The angle $\bar{\beta} = \pm\pi\,(1 - 2d/n)$ and is independent of k_r and k_α.*

PROOF. By Lemma 4, the internal angles of $\{p = n/d\}$ must sum to $n\bar{\psi} = n\pi\,(1 - 2d/n)$. From Lemma 11, for $\xi \in \mathcal{E}_d$, G is a generalized regular polygon $\{p\}$. Therefore, the internal angle $\bar{\psi} = \pm\bar{\beta}$ at each vertex gives $\bar{\beta} = \pm\pi\,(1 - 2d/n)$, independent of k_r and k_α.

With $\bar{\beta}$ independent of the gains k_r and k_α, for a given $\{n/d\}$ formation the corresponding equilibrium value $\bar{\alpha}$ is then determined by equation (8). Thus, the system's steady-state behavior depends only on the ratio k_r/k_α.

5 Local Stability Analysis for $k_r/k_\alpha = k^*$

In this section, for the case when $k_r/k_\alpha = k^*$, we determine which $\{n/d\}$ equilibrium formations are locally asymptotically stable. In this case, according to (5) every point $\xi \in \mathcal{E}_d$ is an equilibrium point of (7). Also, the equilibrium values for $\bar{\alpha}$ and $\bar{\beta}$ are those of Theorem 5.

5.1 Block Circulant Linearization

To facilitate notation, let $q := p^{-1} = d/n$ so that $0 < q < 1$ and is rational. Given that we can write each subsystem (4) more compactly as $\dot{\xi}_i = f(\xi_i, \xi_{i+1})$, its linearization about an equilibrium point $\bar{\xi} = (\bar{\xi}_1, \bar{\xi}_2, \ldots, \bar{\xi}_n)$, $\bar{\xi}_i = (\bar{r}, \bar{\alpha}, \bar{\beta})$ gives n identical linear subsystems, each of the form $\dot{\tilde{\xi}}_i = A\tilde{\xi}_i + B\tilde{\xi}_{i+1}$, where $\tilde{\xi}_i = \xi_i - \bar{\xi}_i$ and the matrices A and B are given by

$$A = \begin{bmatrix} -\frac{1}{2}q\pi\cot(q\pi) & q\pi\bar{r} & \frac{1}{2}q\pi\bar{r} \\ -\frac{1}{2\bar{r}}q\pi & -1 & -\frac{1}{2}q\pi\cot(q\pi) \\ 0 & 1 & 0 \end{bmatrix}$$
$$B = \begin{bmatrix} \frac{1}{2}q\pi\cot(q\pi) & 0 & 0 \\ \frac{1}{2\bar{r}}q\pi & 0 & 0 \\ 0 & -1 & 0 \end{bmatrix}.$$

Therefore, the Jacobian of $\hat{f}$ has the *block circulant* form

$$\hat{A} = \begin{bmatrix} A & B & 0 & \cdots & \cdots & 0 \\ 0 & A & B & 0 & \cdots & 0 \\ \vdots & & & & & \\ 0 & \cdots & \cdots & 0 & A & B \\ B & 0 & \cdots & \cdots & 0 & A \end{bmatrix} =: \mathrm{circ}(A, B, 0, \ldots, 0),$$

where each entry is a 3×3 matrix.

5.2 Equilibrium Subspace

For a given $\{n/d\}$ formation, let $\mathcal{E}_d^0$ denote the invariant subspace formed by $\mathcal{E}_d$, expressed in $\tilde{\xi}$ coordinates; i.e., shifted so that the origin is an equilibrium point $\bar{\xi} \in \mathcal{E}_d$.

Lemma 13 *The restriction of $\hat{A}$ to $\mathcal{E}_d^0$ equals zero.*

In other words, there is a zero eigenvalue in $\hat{A}$ corresponding to motion along $\mathcal{E}_d$. This result is rather obvious, since every point in $\mathcal{E}_d$ is an equilibrium point. Therefore, combining the results of Lemma 9 and Lemma 13, this leaves $3n-4$ eigenvalues of $\hat{A}$, which together determine the local stability properties of a given $\{n/d\}$ equilibrium polygon.

5.3 Block Diagonalization of $\hat{A}$

In this subsection, we demonstrate how the block circulant structure of $\hat{A}$ can be exploited to further isolate its eigenvalues. This is accomplished by block diagonalizing $\hat{A}$. Let $\omega^{i-1} := e^{j2\pi(i-1)/n} \in \mathbb{C}$ denote the i-th of n roots of unity, where $j := \sqrt{-1}$.

Lemma 14 *The matrix $\hat{A}$ can be block diagonalized into* $\mathrm{diag}(D_1, D_2, \ldots, D_n)$*, where each 3×3 block is given by $D_i = A + \omega^{i-1}B$, $i = 1, 2, \ldots, n$.*

The proof of Lemma 14 follows from Theorem 5.6.4 of [5]. Therefore, each diagonal block has the same form

$$D_i = \begin{bmatrix} \frac{\pi}{2} q \cot(q\pi)(\omega^{i-1} - 1) & q\pi\bar{r} & \frac{\pi}{2} q\bar{r} \\ \frac{\pi}{2\bar{r}} q(\omega_{i-1} - 1) & -1 & -\frac{\pi}{2} q \cot(q\pi) \\ 0 & 1 - \omega^{i-1} & 0 \end{bmatrix}.$$

5.4 Main Stability Result

In light of findings from the previous subsection, the eigenvalues of $\hat{A}$ can be further isolated, yielding the following local stability theorem.

Theorem 15 (Local Stability) *For $n > 2$, the only locally asymptotically stable equilibrium polygons are those of the form $\{n/1\}$.*

The proof of Theorem 15 is lengthy and has been omitted due to space restrictions. However, given the block diagonalization of subsection 5.3, the technique for proving Theorem 15 is similar to the proof of Theorem 7 in [13], which pertains to unicycles with constant speed.

Summarizing, for unicycles in cyclic pursuit under the control law (3), with $k_\alpha = 1$ and $k_r = k^*$, formations of the type $\{n/1\}$ with $n \geq 2$ are locally asymptotically stable, while the remaining formations with $d \geq 2$ are not. The equilibrium distance between unicycles $\bar{r} > 0$ depends on the initial conditions. The findings of this section explain the observed simulation results of Fig. 2.

6 Local Stability Analysis for $k_r/k_\alpha \neq k^*$

In this section, we allow the ratio of controller gains k_r/k_α to take on values other than k^*. Again, suppose $k_\alpha = 1$ and $k_r = k$ without loss of generality. In order to make use of the main stability result from the previous section, we only consider the case when $k = k^* \pm \epsilon$, where $\epsilon > 0$. Thus, k remains in some ϵ-neighborhood of k^*. The aim is to (locally) explain the simulation results of Fig. 3 and Fig. 4, where the unicycles converge and diverge, but apparently do so in formation.

Consider a new change of coordinates $\varphi = \Phi(\xi)$,

$$\varphi_1 = r_1, \varphi_2 = \alpha_1 - \bar{\alpha}, \varphi_3 = \beta_1 - \bar{\beta}, \varphi_4 = \frac{r_2}{r_3} - 1, \ldots,$$
$$\varphi_{3n-2} = \frac{r_n}{r_1} - 1, \varphi_{3n-1} = \alpha_n - \bar{\alpha}, \varphi_{3n} = \beta_n - \bar{\beta},$$

so that the last $3n-1$ coordinates are again zero on the affine subspace $\mathcal{E}$, defined in section 4.2. Since $k \neq k^*$, not every point in a given $\mathcal{E}_d$ is an equilibrium point, as in the previous section. Thus, in the new coordinates

$$\begin{aligned} \dot{\varphi}_1 &= -k \left(r_1 \cos\alpha_1 + r_2 \cos(\alpha_1 + \beta_1) \right) |_{\xi = \Phi^{-1}(\varphi)} \\ &= -k\varphi_1 \left(\cos(\varphi_2 + \bar{\alpha}) + (\varphi_4 + 1)(\varphi_7 + 1) \cdots \right. \\ &\quad \left. \cdots (\varphi_{3n-2} + 1) \cos(\varphi_2 + \bar{\alpha} + \varphi_3 + \bar{\beta}) \right), \end{aligned}$$

while the remaining coordinates are such that, if $\varphi_{\mathrm{I}} := \varphi_1$ and $\varphi_{\mathrm{II}} := (\varphi_2, \varphi_3, \ldots, \varphi_{3n})$, we obtain the following upper triangular structure

$$\dot{\varphi}_{\mathrm{I}} = f_{\mathrm{I}}(\varphi_{\mathrm{I}}, \varphi_{\mathrm{II}}) \tag{9a}$$
$$\dot{\varphi}_{\mathrm{II}} = f_{\mathrm{II}}(\varphi_{\mathrm{II}}). \tag{9b}$$

Note that the set of points with $\varphi_{\mathrm{II}} = 0$ exactly corresponds to points in a given affine subspace $\mathcal{E}_d$ and that $f_{\mathrm{II}}(0) = 0$. Thus, if $\varphi_{\mathrm{II}}(t) \to 0$ as $t \to \infty$, the pursuit graph of the unicycles approaches a generalized regular polygon of type $\{n/d\}$, whether the distance between unicycles approaches a constant or not.

Lemma 16 *For a given $\{n/d\}$ formation, the equilibrium point $\varphi_{\mathrm{II}} = 0$ of* (9b) *is locally asymptotically stable for all k sufficiently near k^* if and only if $d = 1$.*

The proof of Lemma 16 follows immediately from Theorem 15. Firstly, from the proof of Lemma 9, we can conclude the Jacobian of f_{II} at $\varphi_{\mathrm{II}} = 0$, denoted A_{II}, has three imaginary axis eigenvalues that are independent of k. Now, it is well known that the eigenvalues of a matrix are continuous functions of its elements. Since the elements of A_{II} are also continuous functions of the parameter $k = k^* \pm \epsilon$, any stable eigenvalues of A_{II} will remain in the left-half complex plane for sufficiently small ϵ. Likewise, any unstable eigenvalues will also remain in the right-half complex plane, implying by Theorem 15 that the only locally asymptotically stable formations are those of the type $\{n/1\}$. In other words, there exists a neighborhood of $\mathcal{E}_1$, wherein $\alpha_i \to \bar{\alpha}$, $\beta_i \to \bar{\beta}$, and the ratio of distances $r_i/r_{i+1} \to 1$. Equivalently, the unicycles converge to a generalized regular polygon formation of type $\{n/1\}$, as per Lemma 11.

The right-hand side of equation (8) defines a function $k(\bar{\alpha})$. Differentiating this with respect to $\bar{\alpha}$ (recall that $\bar{\beta}$ is constant according to Corollary 12) gives

$$\begin{aligned} \frac{\partial k}{\partial \bar{\alpha}} &= \left(\sin\bar{\alpha} + \sin(\bar{\alpha} + \bar{\beta}) \right)^{-2} \\ &\quad \cdot \left(\sin\bar{\alpha} + \sin(\bar{\alpha} + \bar{\beta}) - \bar{\alpha} \left(\cos\bar{\alpha} + \cos(\bar{\alpha} + \bar{\beta}) \right) \right), \end{aligned}$$

which equals $\frac{1}{2}\csc(\pi\frac{d}{n})$ for $\bar{\alpha} = \pm\pi\frac{d}{n}$ and $k = k^*$. Since $\csc(\pi\mu) > 0$ for $\mu \in (0, 1)$, by the continuity of $k(\bar{\alpha})$, the slope of the graph of (8) is positive for k in an ϵ-neighborhood of k^*. Let $\bar{\alpha}$ be the solution to (8) when $k = k^* \pm \epsilon$. Then, for sufficiently small $\epsilon > 0$, $0 < |\bar{\alpha}| = \pi\frac{d}{n} \pm \delta(\epsilon) < \pi$, where $\delta(\epsilon) = \left| |\bar{\alpha}| - \pi\frac{d}{n} \right| > 0$.

Theorem 17 *If $k = k^* - \epsilon$, for small enough $\epsilon > 0$ and $\xi(0)$ in a sufficiently small neighborhood of $\mathcal{E}_1$, the n-unicycle pursuit graph corresponding to (7) converges to a generalized regular polygon of type $\{n/1\}$ while $r_i(t) \to 0$ as $t \to \infty$, $i = 1, 2, \ldots, n$.*

PROOF. By Lemma 16, for a given $\{n/d\}$ polygon, the origin of (9b) is locally asymptotically stable if and only if $d = 1$. Let $\varphi_{\rm II}(t)$ denote the solution of (9b) starting at $\varphi_{\rm II}(0)$. Thus, for $d = 1$ and sufficiently small $\varphi_{\rm II}(0)$ we have that $\lim_{t\to\infty} \varphi_{\rm II}(t) = 0$. Let $\varphi_{\rm I}(t)$ denote the solution of (9a) starting at $(\varphi_{\rm I}(0), \varphi_{\rm II}(0))$. The proof follows by applying Theorem 10.3.1 of [7] to the composite system (9). We first show that the origin of $\dot{\varphi}_{\rm I} = f_{\rm I}(\varphi_{\rm I}, 0)$ is globally asymptotically stable in $\mathbb{R}_+$. Let $V_{\rm I} : \mathbb{R}_+ \to \mathbb{R}$ be the continuously differentiable function $V_{\rm I}(\varphi_{\rm I}) = \varphi_{\rm I}^2/2$, which has the derivative

$$\begin{aligned}\dot{V}_{\rm I}(\varphi_{\rm I}) &= -k\varphi_{\rm I}^2 \left(\cos\bar{\alpha} + \cos(\bar{\alpha} + \bar{\beta})\right) \\ &= -k\varphi_{\rm I}^2 \left(\cos(\pi/n - \delta(\epsilon)) - \cos(\pi/n + \delta(\epsilon))\right).\end{aligned}$$

Since $0 < \pi/n < \pi$, the desired global stability result holds by the Barbashin-Krasovskii theorem [10, Theorem 4.2]. Next, it is required that the $\varphi(t)$ be bounded for all $t \geq 0$. Define the product set $\Omega = \{V_{\rm I}(\varphi_{\rm I}) \leq c_1\} \times \{V_{\rm II}(\varphi_{\rm II}) \leq c_2\}$, where $c_1, c_2 > 0$. The solution $\varphi(t)$ starting at $\varphi(0) \in \Omega$ is bounded for all $t \geq 0$ if Ω is a compact and positively invariant set. Firstly, by a converse Lyapunov theorem [10, Theorem 4.17], there exists a Lyapunov function $V_{\rm II} : \mathbb{R}^{3n-1} \to \mathbb{R}$ for (9b) with the property that $\partial V_{\rm II}/\partial\varphi_{\rm II} \cdot f_{\rm II}(\varphi_{\rm II}) \leq -W(\varphi_{\rm II})$ for sufficiently small $\varphi_{\rm II}$ and where $W(\varphi_{\rm II})$ is a positive definite function. Therefore, $\dot{V}_{\rm II}$ is negative on the boundary $\{V_{\rm II} = c_2\}$ for sufficiently small c_2. The derivative of $V_{\rm I}$ yields

$$\begin{aligned}\dot{V}_{\rm I}(\varphi) \leq -k\varphi_1^2 \big(&\cos(\varphi_2 + \bar{\alpha}) + (\varphi_4 + 1)(\varphi_7 + 1)\cdots \\ &\cdots (\varphi_{3n-2} + 1)\cos(\varphi_2 + \bar{\alpha} + \varphi_3 + \bar{\beta})\big).\end{aligned}$$

Let $\gamma := (\varphi_4 + 1)(\varphi_7 + 1)\cdots(\varphi_{3n-2} + 1)$. Since $0 < \pi/n < \pi$ and because $\varphi_2, \varphi_3 \to 0$ and $\gamma \to 1$ as $\varphi_{\rm II} \to 0$, there exists a neighborhood of $\varphi_{\rm II} = 0$ wherein

$$\begin{aligned}&\cos(\varphi_2 + \bar{\alpha}) + \gamma\cos(\varphi_2 + \bar{\alpha} + \varphi_3 + \bar{\beta}) \\ &\quad = \cos(\tfrac{\pi}{n} - \delta(\epsilon) + \varphi_2) \\ &\qquad - \gamma\cos(\tfrac{\pi}{n} + \delta(\epsilon) - \varphi_2 - \varphi_3) > 0.\end{aligned}$$

Thus, $\dot{V}_{\rm I}$ is negative on the boundary $\{V_{\rm I} = c_1, V_{\rm II} \leq c_2\}$ for any $c_1 > 0$, provided c_2 is chosen small enough. Hence, for any given $c_1 > 0$ and sufficiently small $c_2 > 0$, Ω is a compact positively invariant set. Thus, the trajectories of (9) are bounded for all $t \geq 0$ and $\varphi_{\rm I}(0) \in \mathbb{R}_+$. By Theorem 10.3.1 of [7], $\lim_{t\to\infty} \varphi_{\rm I}(t) = 0$. Or, equivalently, $r_i(t) \to 0$ as $t \to \infty$ for $i = 1, 2, \ldots, n$ (i.e., the unicycles converge to a point).

Theorem 18 *If $k = k^* + \epsilon$, for small enough $\epsilon > 0$ and $\xi(0)$ in a sufficiently small neighborhood of $\mathcal{E}_1$, the n-unicycle pursuit graph corresponding to (7) converges to a generalized regular polygon of type $\{n/1\}$ while $r_i(t) \to \infty$ as $t \to \infty$, $i = 1, 2, \ldots, n$.*

The proof of Theorem 18 is similar to the proof of Theorem 17, except that in the change of coordinates (6), $\varphi_1 = r_1$ is replaced with $\varphi_1 = 1/r_1$. In both cases, computer simulations seem to indicate that the region of convergence for $\mathcal{E}_1$, with respect to variations in the parameter k, is typically quite large. Example simulation results for $k \neq k^*$ are provided in Fig. 3 and Fig. 4, showing how the unicycles converge to a $\{5/1\}$ polygon formation while, at the same time, either converging or diverging, respectively.

7 Conclusion

Following the historical development of cyclic pursuit problems in the mathematics and science literature, this paper presents the results of a local stability analysis for multiple unicycle systems in cyclic pursuit. It is shown that the set of possible equilibrium formations under the chosen pursuit law are generalized regular polygons, and that only those that are *ordinary* (i.e., of the form $\{n/1\}$) are locally asymptotically stable. Moreover, it is shown how changes in the ratio of controller gains can influence the system's overall steady-state behavior. Unfortunately, circular trajectories of fixed radius, such as the one in Fig. 2, occur only for a specific gain k^*, which makes this behavior non-robust from a practical point-of-view. On the other hand, the inputs to each unicycle (r_i and α_i) are ones that could be easily and *locally* implemented on real vehicles. Moreover, in comparison with other circling results found in the literature, our unicycles in cyclic pursuit become ordered and equally spaced along their steady-state trajectories, which is significant from an engineering perspective. Given the robustness issue, a natural question (left to future work) is whether it is possible to make the gain k *dynamic* by employing decentralized feedback towards stabilization to a circle of desired radius. Preliminary work by the authors suggests this is indeed possible. Another extension of this research would be the study of more general pursuit strategies that maintain *circulant* interconnections (e.g., unicycle i pursues both $i + 1$ and $i + 2$), in which case circulant structure could again be exploited.

Acknowledgements

This work was supported in part by the Natural Sciences and Engineering Research Council of Canada (NSERC).

References

[1] F. Behroozi and R. Gagnon. Cylcic pursuit in a plane. *Journal of Mathematical Physics*, 20(11):2212–2216,

November 1979.

[2] A. Bernhart. Polygons of pursuit. *Scripta Mathematica*, 24:23–50, 1959.

[3] A. M. Bruckstein, N. Cohen, and A. Efrat. Ants, Crickets and Frogs in Cyclic Pursuit. Center for Intelligent Systems technical report #9105, Technion-Israel Institute of Technology, Haifa, Israel, July 1991.

[4] H. S. M. Coxeter. *Regular Polytopes*. Methuen & Co. Ltd., London, 1948.

[5] P. J. Davis. *Circulant Matrices*. Chelsea Publishing, New York, 2nd edition, 1994.

[6] V. Gazi and K. M. Passino. Stability analysis of swarms. In *Proceedings of the American Control Conference*, pages 1813–1818, Anchorage, Alaska, May 2002.

[7] A. Isidori. *Nonlinear Control Systems II*. Communications and Control Engineering Series. Springer-Verlag, London, 1999.

[8] A. Jadbabaie, J. Lin, and A. S. Morse. Coordination of groups of mobile autonomous agents using nearest neighbor rules. *IEEE Transactions on Automatic Control*, 48(6):988–1001, June 2003.

[9] E. W. Justh and P. S. Krishnaprasad. Steering laws and continuum models for planar formations. In *Proceedings of the 42nd IEEE Conference on Decision and Control*, pages 3609–3614, Maui, Hawaii, December 2003.

[10] H. K. Khalil. *Nonlinear Systems*. Prentice-Hall, New Jersey, 3rd edition, 2002.

[11] M. S. Klamkin and D. J. Newman. Cyclic pursuit or "The three bugs problem". *The American Mathematical Monthly*, 78(6):631–639, June/July 1971.

[12] J. A. Marshall, M. E. Broucke, and B. A. Francis. A pursuit strategy for wheeled-vehicle formations. In *Proceedings of the 42nd IEEE Conference on Decision and Control*, pages 2555–2560, Maui, Hawaii, December 2003.

[13] J. A. Marshall, M. E. Broucke, and B. A. Francis. Formations of vehicles in cyclic pursuit. *IEEE Transactions on Automatic Control*, 49(11):1963–1974, November 2004.

[14] P. Ögren, E. Fiorelli, and N. E. Leonard. Cooperative control of mobile sensor networks: Adaptive gradient climbing in a distributed environment. *IEEE Transactions on Automatic Control*, 49(8):1292–1302, August 2004.

[15] T. J. Richardson. Non-mutual captures in cyclic pursuit. *Annals of Mathematics and Artificial Intelligence*, 31:127–146, 2001.

[16] T. J. Richardson. Stable polygons of cyclic pursuit. *Annals of Mathematics and Artificial Intelligence*, 31:147–172, 2001.

[17] A. Watton and D. W. Kydon. Analytical aspects of the n-bug problem. *American Journal of Physics*, 37:220–221, 1969.